Check for updates

Hydrogen from wood gasification with CCS – a techno-environmental analysis of production and use as transport fuel†

Cristina Antonini, [ID][a] Karin Treyer, [ID][b] Emanuele Moioli, [ID][c] Christian Bauer, [ID][b] Tilman J. Schildhauer[c] and Marco Mazzotti [ID] *[a]

The use of biomass as a resource for hydrogen production can contribute to the transition towards carbon neutral or carbon negative energy systems. This paper offers a comprehensive investigation of the technical performance and life cycle environmental footprint of three gasification technologies for H_2 production, using dry biomass (wood) as input. These are compared with H_2 production from reforming of natural gas or biomethane and electrolysis as presented in our previous work. This is followed by an evaluation of the use of H_2 as fuel for passenger cars and trucks. The quantity of biomass required for the production of 1 MW H_2 is calculated with an integrated process simulation approach on the basis of Aspen Plus simulations and real-plant literature data. We observe that all the technologies analysed provide negative CO_2 emissions when coupled with CCS. However, the sorption enhanced reforming and the entrained flow gasifiers are more suited to this scope than the heat pipe reformer, because higher overall CO_2 capture rates can be achieved. As CO_2 is from biogenic sources, the life cycle carbon footprint of the produced H_2 is only slightly positive (without CCS) or negative (with CCS). This negative carbon footprint is not obtained at the cost of important trade-offs with regards to ecosystem quality, human health or resource depletion, with the exception of high forest land use. Fuel cell electric vehicles using hydrogen from biomass (both wood and biomethane) with CCS as fuel turn out to be the most climate friendly among all options, with even possible negative total greenhouse gas emissions. However, limited biomass resources and potential alternative uses need to be considered.

1 Introduction

Effective climate change mitigation limiting global warming to 1.5–2 °C in line with the Paris Agreement requires substantial reduction of greenhouse gas (GHG) emissions, aiming for a "net-zero" economy by the middle of this century.[2] This implies a major shift from fossil to renewable primary energy resources in all economic sectors as well as the deployment of negative emission technologies to compensate for GHG emissions difficult to avoid.[2] Hydrogen not only plays a crucial role in an economy compatible with the Paris Agreement, but is also a major player in the EU's commitment to reach carbon neutrality by 2050.[3] Hydrogen is a flexible product and can be used as chemical feedstock, fuel or as energy carrier with many applications in industry, transport and power sectors. Its use does not cause any direct greenhouse gas emissions and offers the co-benefit of zero air pollution as opposed to the centralized and distributed combustion of fossil fuels. However, from an overall system perspective, hydrogen production must be associated with very low GHG emissions in order to contribute to climate change mitigation. This is currently not the case, as the vast majority of hydrogen production relies on fossil feedstock, mainly natural gas and coal.[4] Low-carbon hydrogen production pathways include water electrolysis with low-carbon electricity supply, fossil feedstock conversion with carbon capture and storage (CCS), and biomass conversion, *i.e.* reforming of biomethane (a natural gas equivalent from biogenic origin) or thermochemical conversion of solid biomass.[3] Hydrogen from biomass conversion processes with CCS can even lead to so-called "negative" GHG emissions, *i.e.* permanent removal of greenhouse gases from the atmosphere.[4] The portfolio of "biomass-to-hydrogen" pathways is broad and includes use of different biogenic feedstock, various conversion technologies as well as

[a]*Institute of Energy and Process Engineering, ETH Zurich, Zurich 8092, Switzerland. E-mail: marco.mazzotti@ipe.mavt.ethz.ch*

[b]*Laboratory for Energy and System Analysis, Paul Scherrer Institute, 5232 Villigen PSI, Switzerland*

[c]*Laboratory of Catalysis for Bioenergy, Thermo-Chemical Processes Group, Paul Scherrer Institute, 5232 Villigen PSI, Switzerland*

different alternatives for CO_2 capture and storage.[5–15] To identify the feedstock and conversion options most beneficial for climate change mitigation, these need to be evaluated before large-scale implementation from a technological and environmental perspective employing process simulation, and Life Cycle Assessment (LCA). Quantifying technical and environmental benefits as well as potential trade-offs calls for an assessment of not only hydrogen production, but also of its use compared to conventional (fossil) alternatives.

Techno-environmental assessment of hydrogen from biomass – analyses performed so far

The body of literature addressing technical and environmental aspects of hydrogen production from biomass as such is very broad;[6] however, carbon capture has hardly been included in previous assessments and in general, the majority of the LCA studies reviewed by Tian et al.[6] "failed to explain the robustness (of results) due to the lack of sensitivity and uncertainty analysis, indicating high quality life cycle assessment studies are needed in the future". We recently aimed at partially filling this stated gap by performing a techno-environmental assessment of hydrogen from biomass, focusing on hydrogen production via anaerobic digestion of waste resources with high water content ("wet biomass") and subsequent reforming of bio-methane with and without CCS and compared the results to hydrogen from natural gas reforming and electrolysis.[1] This assessment shows benefits of auto-thermal compared to steam reforming with CCS due to superior CO_2 capture rates, which results in lower life-cycle GHG emissions per unit of hydrogen produced. Furthermore, the use of wet biomass in combination with CCS allows for a net removal of CO_2 from the atmosphere. Hydrogen production using woody (or "dry") biomass via gasification and including CO_2 capture has been evaluated from a techno-environmental perspective by two recent studies.[16,17] Hybrid poplar as feedstock for the gasification process and a low-pressure indirect gasifier consisting of dual fluidised bed (DFB) reactors – the gasifier itself and a char combustor – was evaluated by Susmozas et al.[17] The syngas was fed into a water gas shift (WGS) section involving high- and low temperature shift reactors, followed by a purification section; a pressure-swing-adsorption (PSA) unit is used to separate hydrogen from other gases. CO_2 was captured from the exhaust gas of the boiler with a two-stage gas separation polymeric membrane process. Conversion of Canadian pine wood with two different biomass gasification processes with CO_2 capture was analyzed by Salkuyeh et al.:[16] an atmospheric-pressure, air blown, DFB gasifier, (indirect fired system); and a high pressure, oxygen-blown entrained flow (EF) gasifier (direct fired system). The design of the DFB gasification hydrogen production pathway was similar to the one in Susmozas et al.[17] The EF gasification analyzed required high purity oxygen instead of air as input, thus allowing for a higher process efficiency. The electricity required to run the process auxiliaries and eventually the CO_2 capture unit is provided internally; additional fuel is burned with oxygen to generate process steam via heat integration. This steam is then sent to the power island to produce the electricity

needed. Both studies are based on Aspen Plus simulations and perform a process-based, attributional LCA based on the simulation results. While Salkuyeh et al.[16] reports only LCA results in terms of life-cycle GHG emissions and selected air pollutants, Susmozas et al.[17] quantifies life-cycle GHG emissions, non-renewable cumulative energy demand and selected midpoint impacts applying the CML method.[18] Both studies show negative GHG emissions for hydrogen from biomass gasification with CCS and some trade-offs for other environmental burdens due to CO_2 capture. However, neither of them includes geological storage of CO_2 following CO_2 capture, nor the final use of hydrogen.

Scope and novelty of this study

To the best of our knowledge, we perform the first complete LCA of hydrogen production via gasification of woody biomass with CO_2 capture and permanent geological storage, directly linked to the outcomes of a detailed technical assessment, and its subsequent use as fuel in fuel cell vehicles. This allows for quantification of the environmental benefits and potential trade-offs not only of a broad set of hydrogen production pathways, but also of its application as vehicle fuel compared to other powertrain options. Among the existing gasification technologies we selected the following three wood gasifiers: (i) the heat pipe reformer, (ii) the sorption enhanced reforming, and (iii) the entrained flow gasifier. These three gasifiers differ in terms of process conditions and feedstock pretreatment requirements. Therefore, even if the feedstock used is the same, the composition of the product gas and the amount of electricity required for the operation differ substantially in the three cases. The downstream chain that follows the gasification process is case specific; in fact, the gasifier product gas specifications such as composition, temperature and pressure are different for each gasification technology implemented. Furthermore, we calculate the net energy requirement of the systems by computing the electricity needed by the various process steps and subtracting the electricity co-produced by means of heat integration. In this way it is possible to compare the three technologies in terms of biomass input required for the production of 1 MW H_2, net energy requirements and net CO_2 emissions. The results of the wood-based hydrogen production chains are then compared with the natural gas/biomethane cases studied in our previous work (see Fig. 1 for an overview on the different production pathways considered in this analysis).[1]

The process analysis provides the main indicators required for the integrated techno-environmental modelling framework, which directly connects mass and energy flows from the process simulation with the Life Cycle Inventories (LCI). This integrated approach allows for the quantification of the environmental performance of many different cases based on consistent and physically sound data. The comparative evaluation of hydrogen use in fuel cell electric vehicles (FCEV) and the comparison with other vehicle fuels and drivetrains builds upon recent work of some of the authors, which is particularly valuable for its transparency and completeness.[19,20]

Fig. 1 Schematic representation of all hydrogen production pathways modelled and analysed in this work.

2 Technologies

2.1 Hydrogen production *via* woody biomass gasification

A valuable alternative to classical hydrogen synthesis pathways that involve fossil fuels is the production *via* dry biomass gasification. A variety of gasifiers exists and in the framework of this analysis we selected the following three: (i) the heat pipe reformer (HPR), (ii) the sorption enhanced reforming gasifier (oxySER), and (iii) the entrained flow gasifier (EF) (see Table 1). All the gasification technologies have been tested in relevant fields and have reached a technology readiness level (TRL) higher than 6.

Heat pipe reformer

The HPR technology selected is the one developed primarily at TU Munich, Germany, and continuous operation has been demonstrated at a scale of 500 kW, while the integration of this gasifier in a synthetic natural gas chain has been demonstrated at a scale of 100 kW at the Chair of Energy Process Engineering at FAU Erlangen-Nuremberg, Germany.[21,22] The HPR gasifier is an indirectly heated gasifier that consists of two separated vessels: the gasification reactor and the combustion reactor (see Fig. 2a). Wood is gasified with steam in the gasifier, which is operated at high pressure (feasible upper limit 10 bar).[23] The heat required to perform the endothermic steam gasification reactions is indirectly provided by heat pipes that transfer the heat from the combustor to the gasifier. In fact, char (co-product of the gasification process) and additional wood are

combusted with air in the combustion chamber. Since the two chambers are separated, the syngas produced is almost nitrogen free. The bed material used is Olivine.[24] As shown in Fig. 3a, wood gasification is only one part of the hydrogen production chain. In fact, after the gasification process the product gas needs to be cleaned from particulates and contaminants that could interfere with the downstream processes. After the gasifier, the product gas is cooled down to 823 K before entering the cyclone, where solid particles are separated from the gas. Afterwards, the gas stream enters an hot filter (to eventually get rid of alkali, heavy metals and also remaining particles present in the product gas).[25] To remove the tar from the product gas, different options are available as scrubbing with organic solvents or catalytic reforming. The latter can be performed using a nickel-based catalyst in the form of monoliths as implemented in the SKIVE plant in Denmark.[26,27] Otherwise, a valuable alternative is the combination of a zirconia-based catalyst followed by a second stage with noble metals and/or nickel.[25,28] In the framework of this contribution we opted for a nickel-based catalytic reformer. The operating temperature window of this reactor is between 1123–1193 K;[26] in this contribution we consider that the reactor is operated at 1173 K. Therefore, the product gas is heated up after the hot filter separation. The last step of the gas cleaning section is the desulphurization that consists of two units, a Co–Mo catalytic bed (for COS hydrogenation), and a ZnO catalytic bed with dechlorination agent to remove H_2S and chlorine residues. Before entering the desulphurization section, the product gas is cooled down to 573 K. Afterwards, the cleaned gas is heated up again to 1072 K before entering the steam reformer, where methane is converted into syngas. The molar steam to carbon ratio at the inlet of the SMR is set to 2.6. The reformed gas is cooled down and then shifted in a water gas shift (WGS) section. The molar steam to carbon ratio at the inlet of the high temperature WGS reactor is set to 3.1. After the WGS section the product gas is cooled down (from 685 to 323 K) and then dehydrated and compressed to 26 bar. If the plant is equipped

Table 1 Gasification technologies description

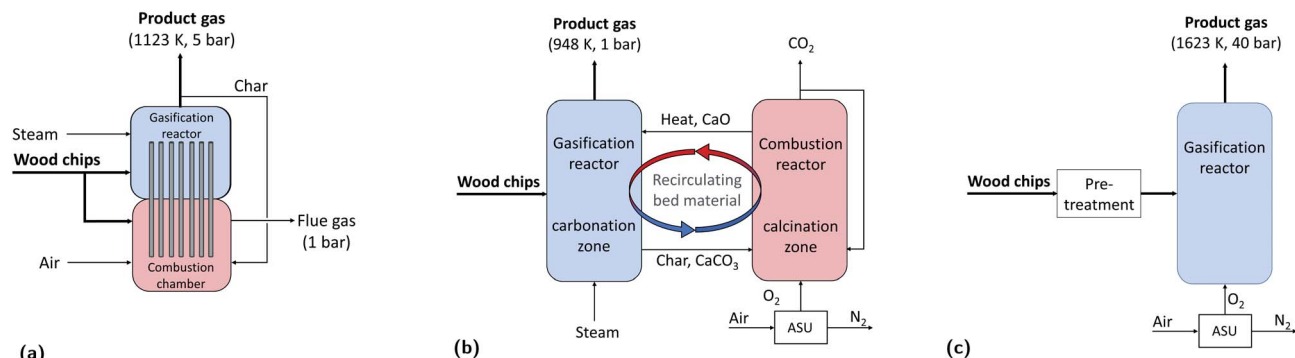| Name	Design	Gasification agent	Heating
HPR	Fluidized bed	Steam	Indirect (air)
oxySER	Fluidized bed	Steam	Indirect (O_2)
EF	Entrained flow	Oxygen	Direct

Fig. 2 Schematic representation of the gasification technologies considered in this work: (a) heat pipe reformer (HPR), (b) sorption enhanced reforming gasifier (oxySER) and (c) entrained flow gasifier (EF).

with a pre-combustion CO_2 capture unit, the CO_2 is separated from the syngas. The raw hydrogen is purified in a pressure swing adsorption (PSA) unit; Hydrogen is obtained with a purity of ≥99.97% and it is compressed to 200 bar, while the rest (also called PSA tail gas) is combusted with air in the SMR furnace. The heat provided by the combustion is needed to perform the endothermic methane reforming reaction. Fig. 3b shows a schematic representation of the hydrogen production chain with the HPR gasifier. A detailed process scheme is available in the Appendix (see Fig. 12).

Sorption enhanced reforming gasifier

The second gasification technology considered is the oxySER gasifier (see Fig. 2b). This technology is a variation of the well-known dual fluidized bed gasifier developed at TU Wien, Austria, which has been tested at a demonstration-plant scale in Güssing, Austria.[29] The sorption enhanced reforming gasifier has been tested at a scale of 100 kW at TU Wien, Austria. It consists of a gasification and a combustion reactor, where limestone ($CaCO_3$) is used as bed material (instead of the standard Olivine). The bed material is recirculating from one bed to the other: limestone is calcined in the combustion reactor and CaO is looped back into the gasification reactor, where it reacts with the CO_2 present in the product gas, leading to *in situ* CO_2 capture.

$$CaO + CO_2 \rightleftharpoons CaCO_3 \qquad (1)$$
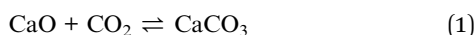
The removal of CO_2 shifts the equilibrium of the WGS reaction towards the products, therefore the volumetric content of H_2 in the syngas is very high (*ca.* 70%). The char produced during the gasification process is transported with the bed material from the gasifier to the combustion reactor where it is combusted with oxygen. A CO_2-rich stream is collected at the outlet of the combustion reactor and then dehydrated and compressed to be suitable for geological storage. To control the temperature in the combustion chamber, part of the CO_2 is recirculated back in the combustor. The O_2 needed in the combustion process is produced by an air separation unit (ASU). As for H_2 production from a HPR gasifier, the product gas has to be cleaned and desulphurized, where the same cleaning procedure and downstream train as for

the HPR production chain are considered. Fig. 3b shows a schematic representation of the hydrogen production chain with the oxySER gasifier; a detailed process scheme is available in the Appendix (see Fig. 13).

Entrained flow gasifier

The third gasification technology is a pressurized entrained flow gasifier (Fig. 2c). This technology is widely used at industrial-scale (in plants of more than 100 MW_{th}) for coal gasification in integrated gasification combined cycles (IGCC) and for chemical synthesis applications. Furthermore, the co-gasification of biomass in large scale IGCC has already been tested.[30,31] In contrast to fluidized bed gasification, where the wood chips are directly fed into the gasification reactor, a thorough pre-treatment is needed. Here we consider pre-drying, torrefaction and pulverisation (to reach an average particle size smaller than 0.5 mm) as suggested in Tremel *et al.*[32] A pressurized feeding system is needed and different technologies are available; we select as reference technology the hydraulic piston system with screw feeding.[33,34]

The product gas is treated in a gas cleaning section; first, it is cooled down to 873 K before the cyclone, where solids particles are separated from the gas. Then, the gaseous stream is further cooled down at 573 K before entering the candle filter. Because of the elevated temperature reached in the gasifier, the product gas contains neither tar nor methane hence tar catalytic reforming and steam reforming are not required. Therefore, after the candle filter, the gaseous stream is sent to the desulphurization unit. After the cleaning section, the hydrogen yield has to be increased, and because of the large amount of carbon monoxide present in the product gas, a water–gas shift section with two reactors, one at high and one at low temperature, is required. The shifted syngas can be sent to the CO_2 capture plant or directly to the purification unit (see the schematic representation of the process in Fig. 3c). A detailed process scheme is available in the Appendix (see Fig. 14).

In all hydrogen production chains, process steam is co-produced by means of heat integration; some of it is used in the process, while the rest is expanded in a turbine section (information on power island are available in the ESI†). The

electricity produced is used internally to run the various utilities, and in case of excess it is fed into the grid. Concerning the CO_2 capture unit, an amine-based absorption process is considered, where the solvent used is methyl diethanolamine (MDEA). The CO_2 capture rate selected is 98%.

2.2 Hydrogen production *via* natural gas/biomethane reforming with carbon capture and storage

Steam methane reforming (SMR) and autothermal reforming (ATR) of natural gas (NG) and biomethane were described and investigated in our previous work.[1] In this analysis we compare

the technical and environmental performance of producing hydrogen from wet waste biomass converted to biomethane (see Fig. 1) with the benchmark production *via* NG reforming. We consider biomethane as a starting point for the comparison and neither biogas nor wet biomass because of the following reasons: first of all the availability of wet biomass is generally decentralized at small scale, and second, the transport of both, precursor (wet biomass) and product (biogas), is challenging. Therefore, we believe that it is generally convenient to produce and upgrade biogas to biomethane locally and then feed it into the natural gas grid. Therefore, what we are presenting here as "H$_2$ production *via* biomethane reforming", corresponds to
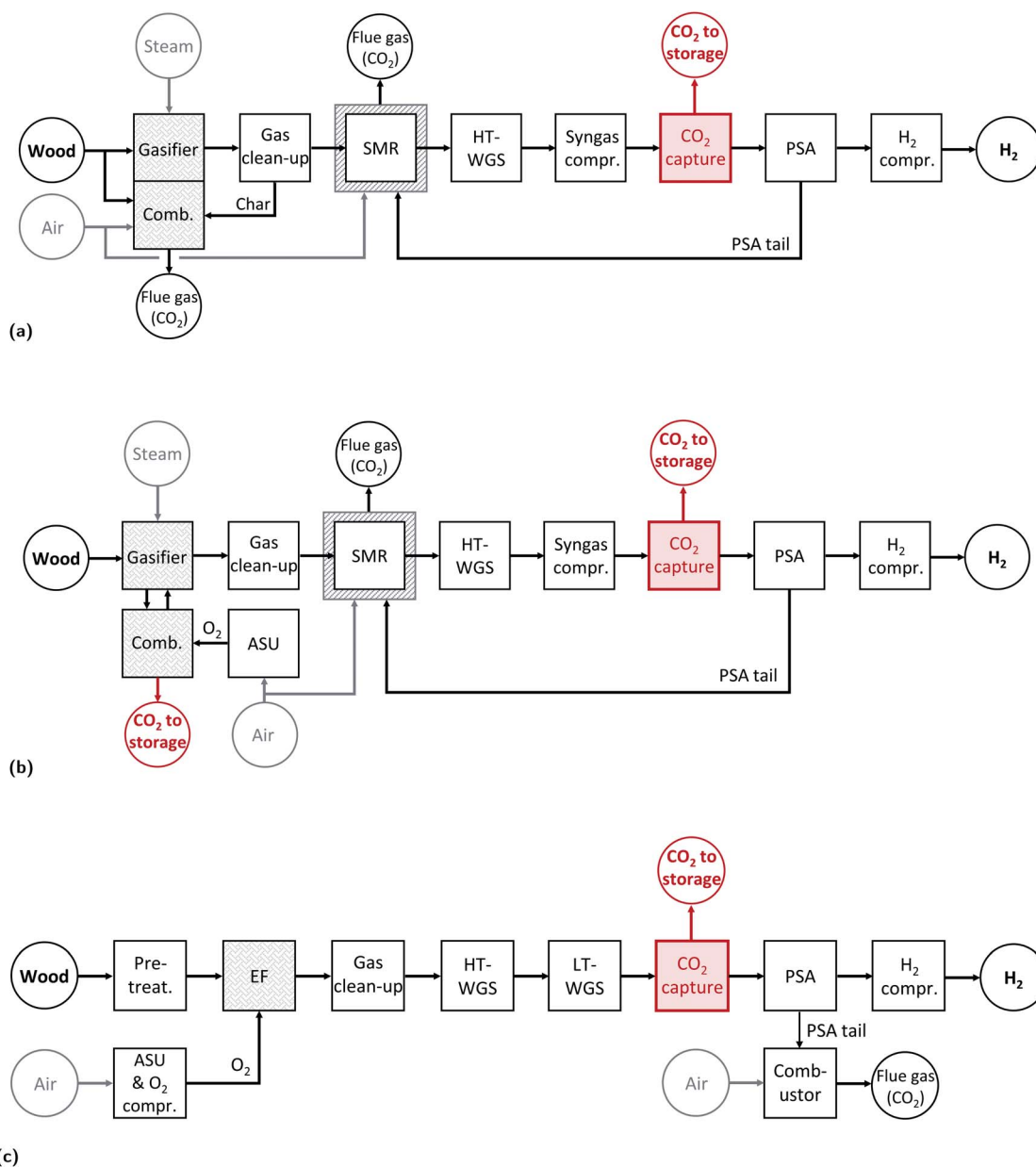

Fig. 3 Wood to hydrogen production chains: (a) with a HPR gasifier, (b) with an oxySER gasifier, and (c) with an EF gasifier. All three production pathways have been analysed with and without the option of capturing and storing CO_2. Therefore, in case no CCS is applied, the production chain remains the same with the absence of the red CO_2 capture unit. HT/LT-WGS: high/low temperature water–gas shift reactor; PSA: pressure swing adsorption unit; ASU: air separation unit.

a hypothetical case where the plant is 100% fed with biomethane.

3 Process modelling

In this section a detailed description of the process modelling strategy is provided. The functional unit is "production of 1 MW of hydrogen, with purity of at least 99.97%". To be precise, for the configurations including an EF or an ATR unit, argon (Ar) is introduced into the system as an impurity of the oxygen stream. Argon is a light inert gas, it does not interfere with any conversion or purification process but it leaves the system with the purified H_2 stream. To distinguish between Ar and the rest of the impurities (*i.e.* CH_4, CO, CO_2 and N_2) we define an "adjusted purity" where Ar is not taken into consideration. Therefore, for all EF and ATR cases we consider an adjusted purity of at least 99.97%, which correspond to an overall purity of at least 99.9%. As feedstock we consider forest wood chips with a molecular composition in line with the LCA according to the ecoinvent report on wood energy:[35] C 49.4 wt%, O 44.5 wt% and H 6.1 wt% (LHV of 18.9. MJ kg^{-1}).

3.1 HPR and oxySER gasifiers

Given the complexity of the fluidized bed gasifiers (HPR and oxySER), we adopted a so called "black-box modelling approach"; based on data available in the literature we define a base-case product gas composition (see the ESI† for data and references). Starting from these compositions, we calculate the product gas flow rate needed to produce 1 MW of H_2. For the HPR we assume that 33% of the total biomass input is combusted in the combustion chamber.[21–23] While for the oxySER we assume that 63 mol% of the carbon present in the biomass is burnt in the combustor.[36,37] The amount of steam needed as reactant is subtracted by the amount of process steam co-produced; whereas the remaining process steam is expanded in the turbine section. The oxygen used in the oxySER and EF gasifiers is assumed to have a purity of 99.5%, with the make-up being argon, and an energy consumption of 265 kW h per ton O_2 is considered (see the ESI† for calculations and modelling assumptions).[38,39]

3.2 EF gasifier

Contrary to the other two gasification technologies, in this case the biomass needs to be pre-treated. Hence, we consider the following pre-treatments: pre-drying, torrefaction and pulverization. Instead of modelling these processes in detail we assign the corresponding energy consumption based on data available in the literature (see ESI† for more details).[32,40] The EF gasifier is modelled in Aspen Plus V 8.6, following the modeling strategy presented in Meerman *et al.*[33] The gasifier is operated at 40 bar and isothermally at 1623 K. The molar oxygen to carbon (O/C) ratio is 0.32 and O_2 is fed with an over-pressure factor of 1.2 (48 bar); the compression of oxygen occurs in 4 steps with an intercooling temperature of 308 K. The calculations and modelling assumptions are described in the ESI.†

Table 2 Sensitivity analysis; pp: percentage points, dBM: dry biomass

Parameter	Base case	Range of sensitivity
HPR		
γ_W [%]	33	±2 pp
η_G [%]	70	±4 pp
oxySER		
γ_C [%]	63	±2 pp
EF		
γ_{dtp} [%]	5	±2.5 pp
ω_{dtp} [kWel kg$_{dBM}$$^{-1}$]	0.128	± 20%

3.3 Reforming of biomethane

The reforming-based technologies considered in our comparative evaluation (SMR and ATR of natural gas and biomethane) have been comprehensively described in our previous publication.[1]

3.4 Sensitivity analysis

Wood gasification is a complex process and, as explained in the previous section, for some of the technologies we used literature data instead of developing a detailed physical model. To assess the dependency of the results on the modelling assumptions and to offer a better overview on the effect of parametric variation on the process outputs, we performed various sensitivity analysis (see Table 2 for the details). First of all, based on the results available in the literature, we defined a range of possible compositions of the product gas of both HPR and oxySER gasifiers; as lower bound (LB) we defined the composition with the lowest energy content (LHV-based), while as upper bound (UB) the one with the highest (see ESI† for data and references). For the HPR configurations we perform a multi-parameter sensitivity analysis; the two parameters selected are the gasifier efficiency (η_G) and the amount of wood combusted in the combustion chamber (γ_W). The gasifier efficiency is defined as the ratio between the energy content of the product gas and the energy content of the wood inlet (LHV-based):

$$\eta_G = \frac{LHV_{PG} m_{PG}}{LHV_{wood} m_{wood}} \quad (2)$$

while γ_W is defined as the ratio between the amount of wood sent to the combustion chamber and the overall wood inlet:

$$\gamma_W = \frac{LHV_{wood} m_{wood}^{comb}}{LHV_{wood} m_{wood}^{tot}} \quad (3)$$

For the oxySER configurations we performed a sensitivity analysis on the percentage of carbon that is consumed in the combustion chamber (γ_C), defined as the molar ratio between the moles of carbon in the combustor flue gas n_C^{cFG} and those present in the biomass inlet stream (n_C^{dBM}):

$$\gamma_C = \frac{n_C^{cFG}}{n_C^{dBM}} \quad (4)$$

In the case of the EF gasifier, the section that is not modelled in detail is the biomass pre-treatment (comprising drying, torrefaction and pulverisation). Therefore, we performed a multi-parameter sensitivity analysis on two parameters: on the energy consumption of these processes (ω_{dtp}) and on the amount of biomass lost during the pre-treatment (γ_{dtp}). The energy consumption is defined as the kW of electricity needed per kg of dry biomass processed:

$$\omega_{dtp} = \frac{E_{dtp}}{m_{dBM}} \qquad (5)$$

while γ_{dtp} is defined as the percentage of biomass lost (dry basis) during pre-treatment.

4 Life cycle assessment

The evaluation of the environmental performance of potential near-future Negative Emission Technologies (NET) needs to consider a life cycle perspective taking into account all environmental burdens occurring during the entire life cycle of a product or service.[41] We perform an ISO 14040 [42] and 104044 [43] compliant, attributional Life Cycle Assessment (LCA) of the production of 1 MJ H_2 via gasification of woody biomass at a pressure of 200 bar and a purity higher than 99.97% (SMR, HPR and oxySER) or higher than 99.9% (ATR and EF, with argon representing the additional impurity). Calculations are performed with the open-source software Brightway2 [44] and the ecoinvent life cycle inventory database v3.6, system model "allocation, cut-off by classification".[45] All Jupyter notebooks and detailed Life Cycle Impact Assessment (LCIA) results are

part of the ESI.† The system boundaries and allocation choices are illustrated in Fig. 4, and the geographical scope is Europe. The wood chips used as feedstock for gasification are a product from sustainable softwood and hardwood forestry of various species grown in Germany and Sweden (namely beech, birch, oak, pine and spruce), which represent the European market for wood chips in ecoinvent v3.6. It should be noted that the carbon uptake is assumed to be the same for all these species in ecoinvent. Other variabilities in terms of forestry in other European countries, transport distances, regional market compositions, or wood imports from overseas could not be modelled within the scope of this paper due to lack of information. All carbon content values are calculated on a dry matter basis. Carbon uptake by trees is accounted for with a characterisation factor of −1 for CO_2, while release of biogenic CO_2 is accounted for using a positive factor of 1 in order to be able to quantify impacts on climate change due to capturing and permanently storing biogenic CO_2. Detailed discussion of the carbon balance of the biomethane chain and corresponding modeling choices are part of our previous work.[1] Impacts on climate change of greenhouse gases are quantified according to the IPCC 2013 LCIA method with a 100 years Global Warming Potential timeframe[2] as implemented in the ecoinvent database. The ILCD 2.0 (2018) LCIA method[46] covering environmental impacts such as ecotoxicity, effects on the human health, ozone layer depletion or near-ground photochemical ozone creation, or metal depletion is further used, in addition to the non-renewable cumulative energy demand (CED) as a measure for depletion of fossil, nuclear and non-renewable forest resources. The inventories for the natural gas supply
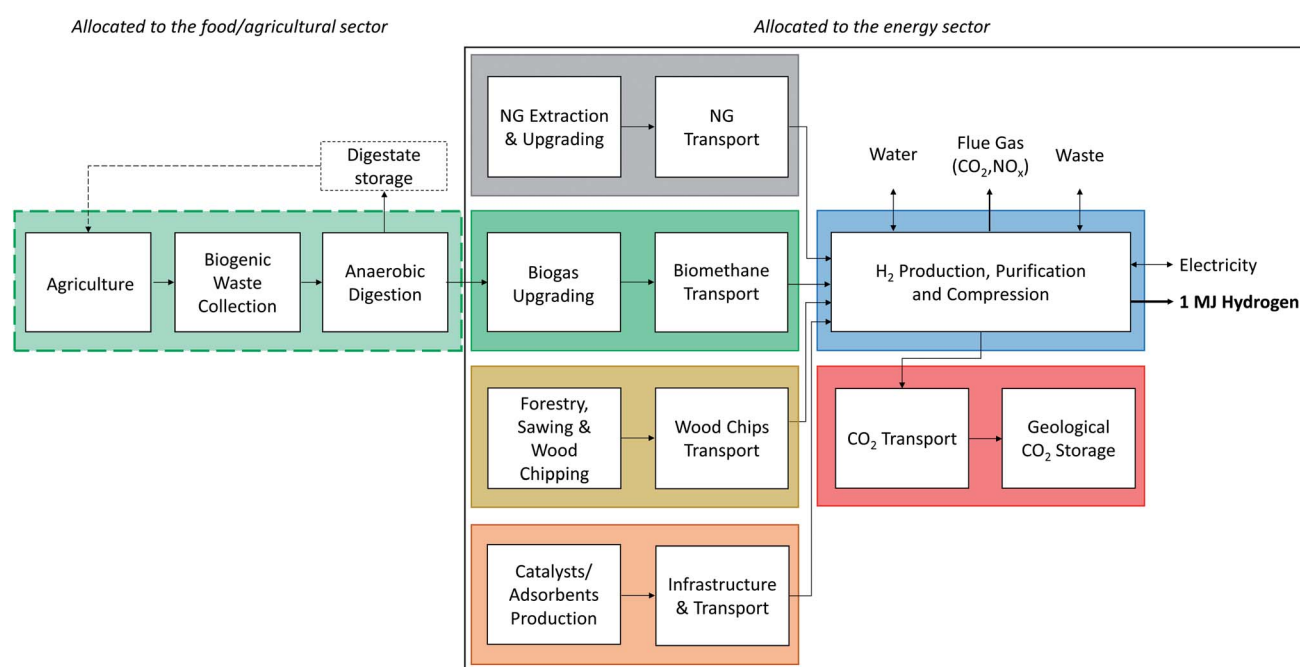

Fig. 4 System boundaries chosen for the LCA of H_2 production from natural gas (NG), biomethane, or wood as feedstock. The chain of the wet waste biomass down to the by-product biogas from treatment of the wet waste biomass in an anaerobic digestion plant is allocated to the food and agriculture sector. Extended from our previous work.[1]

chain as well as all materials, infrastructure, or transports (*i.e.* the life cycle inventories of the so-called "background processes") are taken from the ecoinvent database, while the biomethane chain, H_2 production plant, and CO_2 transport over 200 km per pipeline and storage in a saline aquifer at a depth of 800 m are all based on data from previous analyses of the authors or own project-specific data. Electricity use or electricity fed back to the grid in case of excess electricity is modelled with the European ENTSO-E mix as default option; however, we also perform sensitivity analysis and show the effect of varying the greenhouse gas intensity of electricity on climate change impacts of hydrogen production by extending a figure we already provided earlier;[1] we now include wood gasification in addition (see Fig. 15).

Our analysis of the use of hydrogen is limited to its application as vehicle fuel. We build upon previous work performed by some of the authors[19,20] and link the hydrogen production pathways modeled within this analysis and our previous work[1] to vehicle (LCA) models established by Sacchi *et al.*[19,20] to quantify life-cycle environmental burdens of passenger vehicles and trucks with different hydrogen supply options for FCEV compared to conventional gasoline and diesel vehicles as well as battery electric vehicles (BEV). Such modelling of the end use enables understanding the importance of differences in LCIA scores of the various H_2 production pathways from an overall LCA perspective.

5 Results and discussions

The technical performance of the different hydrogen production pathways is evaluated based on four key indicators: product gas molar composition (Fig. 5), overall CO_2 capture rate (Fig. 6b), electricity balance (Fig. 7) and net process efficiency. The overall CO_2 capture rate is the ratio between the amount of CO_2 captured and the overall CO_2 produced (sum of the CO_2 captured and emitted). The electricity balance includes the overall electricity consumption of the H_2 production plant, normalized by the amount of H_2 produced (which is constant for all cases presented), while the net process efficiency is defined as the energy content of hydrogen produced, divided by the energy content of the biomass needed to produce it. In Fig. 8 the conversion of wood into hydrogen is compared with natural gas/biomethane reforming. The presentation of the LCA results is structured as follows. First, climate change impacts from the six configurations modelling the gasification of wood are compared to selected configurations for hydrogen production *via* steam methane reforming or autothermal reforming of natural gas or biomethane with and without CCS[1] (Fig. 9). Then, we provide a comparison of the performance of the various H_2 production pathways with regards to selected Life Cycle Impact Assessment (LCIA) categories (results for all LCIA categories are included in the ESI†) (Fig. 10). Finally, the use of H_2 in fuel cell passenger cars and trucks is compared with other fuel supply and vehicle options in terms of impacts on climate change (Fig. 11) (all LCIA categories represented in the ESI†). Fig. 15 in the appendix expands an already published figure with the gasification cases to show the sensitivity of the climate change
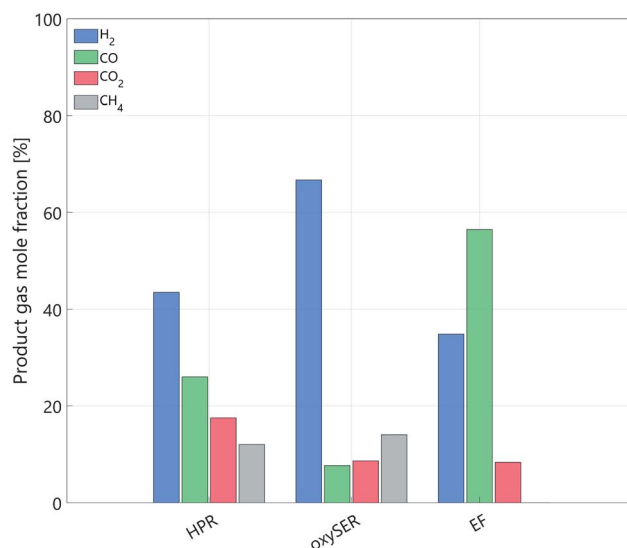

Fig. 5 Gasifiers product gas molar composition after the gas cleaning section; HPR and oxySER: base case product gas composition.

impacts of H_2 production on the greenhouse gas intensity of input electricity.

5.1 Gasifiers product gas composition

Fig. 5 shows the product gas molar composition of the three gasifiers after the gas cleaning section; for the HPR and oxy-SER gasifiers the composition refers to the base case. The base-case cleaned product gas of the HPR gasifier contains around 44 mol% of hydrogen, 26% of CO, 18% of CO_2, and around 12 mol% of methane. Methane is converted *via* reforming into syngas (CO and H_2), and to increase the H_2 yield, carbon monoxide is shifted with steam in a WGS section. The oxySER product gas is richer in hydrogen (base-case composition 67 mol%). However, because of the low operating temperature of the gasifier, a substantial amount of methane is generated (*ca.* 14 mol%, which corresponds to almost 10 wt%), which is converted into syngas *via* steam reforming. Therefore, although the molar fraction of CO present in the product gas is relatively low (below 10 mol%), it increases after the reforming process and therefore, to raise the H_2 yield, a WGS section is needed. The product gas after the EF reactor contains a substantial amount of CO (*ca.* 60 mol%); this is because oxygen is used as gasification agent instead of steam. Therefore, a WGS section with two reactors (at high and low temperature) is needed. The advantage of the EF reactor is that, by operating the gasifier at high temperature (>1600 K), the product gas is free of hydrocarbons (*i.e.* methane and tar).

5.2 Net efficiency and sensitivity analysis on the carbon balance

Fig. 6a shows the net efficiency and the corresponding overall CO_2 capture rate of the different wood to hydrogen production chains. The results of the sensitivity analysis are enclosed in the range delimited by the transparent area, while the specific

Fig. 6 (a) Comparison of the net efficiency (left y-axis, black dots and gray areas) and of the overall CO_2 capture rate (right y-axis, red diamonds and areas). (b) This figure shows the specific CO_2 captured and emitted in each production chain. For the HPR and oxySER cases the bar corresponds to the base case, while the error bar highlights the variation due to the sensitivity analysis on different parameters and product gas composition.

results for the base case are shown with black dots (net efficiency) and red diamonds (CO_2 capture rate). Fig. 6b instead shows the specific amount of CO_2 captured (in red) and emitted (in gray); the error bar highlights the variation due to the sensitivity analysis on different parameters and to the different product gas compositions tested (lower bound, base case and upper bound).

The net efficiency of the HPR configurations ranges from 58 to 65%, and if a pre-combustion capture plant is added to the chain, the overall CO_2 capture rate goes from 0 to *ca.* 60%. Focusing on the impact of the sensitivity analysis, we can say that the variation of γ_W affects both the net efficiency and the specific CO_2 emissions. Indeed, the less wood goes to the combustor (γ_W smaller) the less CO_2 is emitted per unit of hydrogen produced. This translates into higher efficiency and lower specific carbon emissions. The net efficiency is also affected by the variation of η_G; the more efficient the gasifier, the less wood is required per unit of H_2 produced. Finally, the variation in the specific CO_2 captured is due to the different product gas compositions tested (LB, BC and UB).

The net efficiency of the oxySER configurations without and with the addition of a CO_2 capture plant (oxySER S and oxySER CCS, respectively), ranges from 60 to 82%. Unlike the HPR cases, the range of variability is remarkable and it is due to the uncertainty on both product gas composition and amount of carbon entering the combustor. The variation on the net efficiency from the base case composition to the lower/upper bound cases is around ±7 pp. Additionally, by varying γ_C by ±2 pp, the net efficiency in all three cases (BC, LB and UB) varies by ±4 pp. Based on these results we can conclude that the performance of the oxySER configurations strongly depends on the operating conditions of the gasifier (*i.e.* temperature and residence time). As already explained in Section 2.1, because of the oxy-fuel combustion, CO_2 can be recovered at the outlet of the combustion reactor without the

need of a dedicated capture unit. Therefore, if we dry, compress and store the CO_2-rich stream produced by the combustor, we can reach a similar overall capture rate as the configuration with a HPR gasifier with pre-combustion capture (*ca.* 60%). Whereas by adding a pre-combustion capture plant (oxySER CCS) we can capture also the CO_2 present in the syngas, reaching an overall CO_2 capture rate of *ca.* 92%. The remaining CO_2 is emitted in the flue gas resulting from the combustion of the PSA tail gas (see Fig. 3b). As shown in Fig. 6b, the variation of γ_C affects the amount of CO_2 captured. However, its effect on the overall CO_2 capture rate is larger for the oxySER S than for the oxySER CCS configuration, because while applying a dedicated pre-combustion capture unit the perturbation on γ_C only affects part of the total CO_2 captured.

The highest overall CO_2 capture rate is reached by the configuration with an EF gasifier with CCS (*ca.* 98%); concerning the net efficiency both EF and EF CCS cases perform slightly worse than the other configurations; indeed, they require more wood per unit of hydrogen produced. The net efficiency of the two EF configurations is affected by the sensitivity analysis on γ_{dtp}; the less dry mass is lost during the pre-treatment, the more efficient is the overall process. However, as shown by the gray area in Fig. 6a, the variation is limited.

5.3 Analysis on the specific electricity consumption

Fig. 7a shows the net efficiency and the electricity balance for all configurations; when the net electricity balance is below zero, electricity has to be provided to the system. Fig. 7b shows the specific electricity balance of the six configurations (only the base cases are considered) divided into ten categories: CO_2 compression, CO_2 capture, H_2 compression after the PSA unit to 200 bar, H_2 production plant auxiliaries (pumps, blower,…), syngas compression before the separation/purification section, air separation unit (ASU), O_2 compression, biomass

Fig. 7 (a) Comparison of the net efficiency (left *y*-axis, black dots and gray areas) and of the electricity balance (right *y*-axis, light blue squares and areas), of all hydrogen production configurations from dry biomass. (b) Specific electricity consumption of the wood to hydrogen production chains; the red triangle shows the net amount of electricity (in kW) that has to be supplied from the grid per MW of hydrogen produced.

feed pressurization, biomass pre-treatment, and electricity co-produced.

In general, the addition of a CO_2 capture plant results in an additional energy demand, proportional to the amount of CO_2 captured; both electricity and heat are needed to run the CO_2 capture plant and the dehydration and compression section. The oxySER CCS and EF CCS configurations are the most energy demanding. In the case of the oxySER, the variation on the electricity balance shown by the blue shaded area is mainly due to the variation on γ_C: the less carbon goes to the combustor, the less CO_2-rich flue gas is produced and therefore less CO_2 is dehydrated and compressed. Consequently, it results in a reduction of the energy demand.

Whereas for the EF and EF CCS, the variation in the net electricity balance is due to the uncertainty on the amount of biomass pre-treated (the bigger the dry mass lost due to pre-treatment, the more biomass has to be pre-treated per unit of hydrogen produced) and on the energy consumption of the different pre-treatment processes (ω_{dtp}).

As shown in Fig. 7b, the electricity required to compress the hydrogen delivered by the PSA unit to 200 bar is more or less equal for all six cases. Focusing on the configuration with a HPR gasifier without CCS, we notice that the electricity balance is driven by the electricity required for syngas compression. If we add CCS, we can capture around 60% with an electricity consumption increase of around 65%. Regarding the oxySER configurations we also have to account for the electricity consumed by the air separation unit. The majority of the carbon (63 mol%) goes to the oxy-combustion chamber, and thus also in the configuration without CCS (oxySER S), the electricity required for CO_2 compression is significant. By adding CCS we can increase the capture rate from 63 to 92% of the overall direct CO_2 emissions, which corresponds to an increase on electricity consumption of about 20%.

The configurations with an EF gasifier instead require considerably less electricity to run the hydrogen production plant; indeed, the system is operated under pressure and no compression of the syngas before the purification section is needed. However, they require extra electricity for biomass pre-treatment, O_2 compression and biomass feed pressurization. While adding CCS, because of the single-reactor configuration, an overall CO_2 capture rate of about 98% can be obtained; nevertheless, the electricity consumption increases (it corresponds to *ca.* 153% of the case without CCS).

5.4 Comparison between hydrogen production from wood, natural gas and biomethane

Fig. 8 illustrates the comparison between the hydrogen production chains from wood and natural gas/biomethane. With the exception of the two configurations with an oxySER gasifier, the net efficiency is higher when using natural gas or biomethane as feedstock. The origin of this variation lies in the different C/H ratio in biomass with respect to methane (1 : 1.5 *vs.* 1 : 4). Excluding the oxySER upper bound cases, gas/biomethane production chains are performing better in terms of net efficiency and overall electricity balance; in fact, the amount of energy input to the production chain (both feedstock and external electricity from the grid) is considerably higher for the wood cases. However, in order to draw some final conclusions we have to look at the whole life cycle analysis of the different chains.

5.5 Climate change and other environmental impacts of hydrogen production from wood compared with reforming of natural gas or biomethane and electrolysis

Based on the technical modelling results discussed in the previous sections, the life-cycle environmental impacts of H_2 production from wood gasification in the configurations HPR, oxySER and EF with and without CO_2 capture and storage have

Fig. 8 Comparison of the net efficiency (black) and the electricity balance (light blue) between wood and natural gas/biomethane H_2 chains. The light-blue dotted line illustrates the 0 value for the electricity balance: all cases that are below this threshold have to import electricity while the cases that are above have electricity in excess to be fed into the grid.

been calculated. Results are compared to the environmental impacts of H_2 production from reforming of natural gas or biomethane as well as from electrolysis with varying electricity sources as described in our previous work.[1] Impacts on climate change from H_2 from electrolysis are inherently linked to the greenhouse gas intensity of the electricity used for the process, which is shown in Fig. 15 in the appendix. A similar figure has already been provided in our previous work[1] and has now been extended to include the gasification of wood.

Fig. 9 shows the contribution of different life cycle phases to the overall impact on climate change per MJ of H_2 produced. Further, it shows the overall CO_2 capture rate at the hydrogen production plant. The feedstock supply of wood gasification processes, *i.e.* forestry and wood chipping, comes with net negative emissions from biogenic carbon uptake by trees even when GHG emissions from forestry, transportation, energy use for the chipping, *etc.* are considered. Due to the low H/C ratio of wood, a rather large amount of wood chips is required as feedstock to produce 1 MJ H_2, which leads to both a rather high amount of CO_2 removed from the atmosphere through the fuel supply, but also to high direct biogenic CO_2 emissions in cases without CCS. The HPR and the EF process chains without a pre-combustion CO_2 capture unit exhibit slightly positive impacts on climate change (16 g and 14 g CO_2-eq per MJ hydrogen, respectively). This is due to the electricity required, assumed to be provided by the European grid, which is associated with life cycle GHG emissions of about 400 g CO_2-eq per kWh. OxySER S exhibits negative emissions (*ca.* −70 g CO_2-eq per MJ) even without a pre-combustion carbon capture unit, thanks to the oxy-combustion process and the possibility to permanently store CO_2 even without a dedicated carbon capture unit. Even though the oxySER S configuration requires comparatively high amounts of electricity, the CO_2 emissions related to the

use of electricity are more than compensated by the CO_2 captured from the combustion unit, when subsequent CO_2 transport and storage is assumed (see Section 2.1 for the technology description).

When one considers the same H_2 production chains with pre-combustion carbon capture, the overall GHG emissions become negative in all the cases (between −70 g CO_2-eq per MJ for HPR CCS and −143 g CO_2-eq per MJ for EF CCS). The impacts of the carbon capture, transport and storage processes on the results are negligible, so that the fuel supply chain, CO_2 capture rate and power balance at the plant are decisive. Therefore, the addition of CCS leads to a substantially improved performance of all the process chains analysed with respect to overall greenhouse gas emissions.

Compared to other hydrogen production pathways, wood gasification performs well in terms of impacts on climate change. As Fig. 15 shows, electrolysis operated with renewable electricity generates hydrogen with life-cycle GHG emissions in the order of almost zero (with hydropower) to about 50 g CO_2-eq per MJ (with electricity from photovoltaic arrays). Natural gas reforming causes impacts on climate change in a range from about 90 g CO_2-eq per MJ in the case of ATR and SMR w/o CCS down to 20 g CO_2-eq per MJ for ATR with CCS. Using biomethane as input to the same reforming processes decreases the life-cycle GHG emissions to 10 g CO_2-eq per MJ (assuming low carbon uptake into biomass and digestate incineration) without CCS, going negative with CCS to −120 g CO_2-eq per MJ in the best case. For a detailed discussion of hydrogen from natural gas and biomethane reforming, we refer to our previous analysis.[1] However, the generally observed trend that wood gasification with CCS generates more negative emissions than biomethane reforming with CCS can be attributed to to the lower H/C ratio of wood compared to methane and to the lower process efficiency, which lead to higher removal of CO_2 per unit of hydrogen for
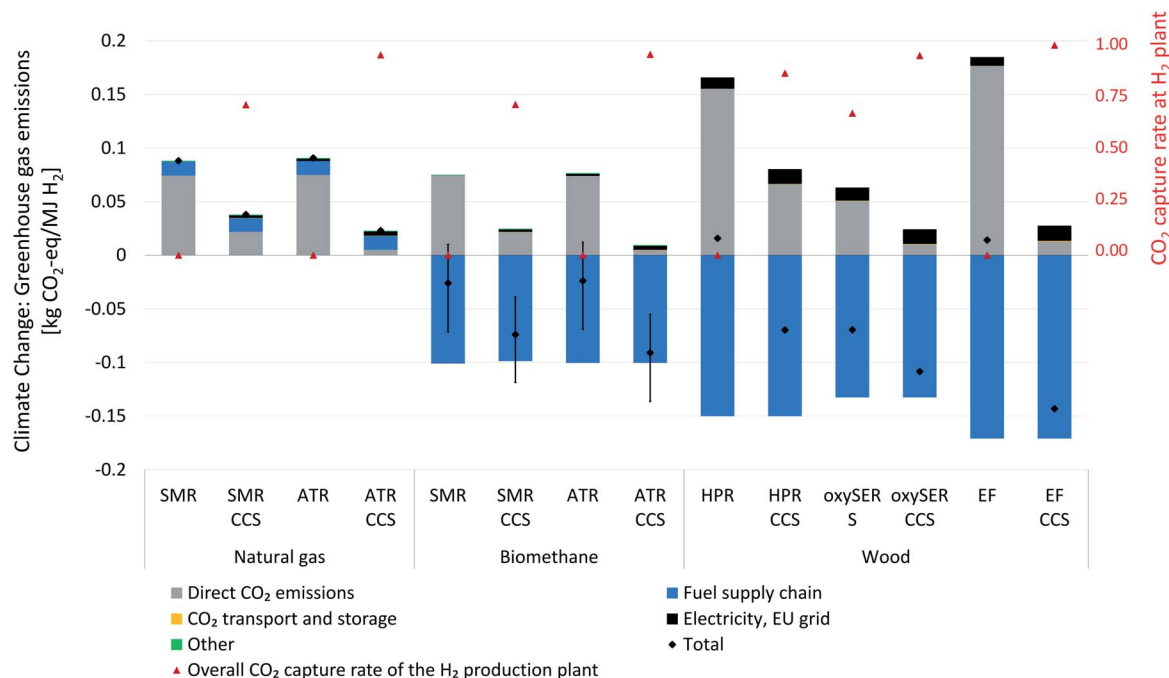
Fig. 9 Contribution of life cycle phases to the impacts on climate change from production of 1 MJ H_2 at 200 bar *via* selected technologies and system designs. The right *y*-axis shows the overall CO_2 capture rate at plant level. The category "Other" includes "Catalyst and Adsorbents", "Direct emissions from fuel combustion in furnace", "H_2 production unit infrastructure", and "Water supply".

Fig. 10 Performance of selected individual hydrogen producing technologies in selected impact categories per MJ of hydrogen. Scores are normalised to 1, which corresponds to the maximum score in each impact category, *i.e.* the technology which performs worst on the positive scale or, in the case of climate change, best on the negative scale.
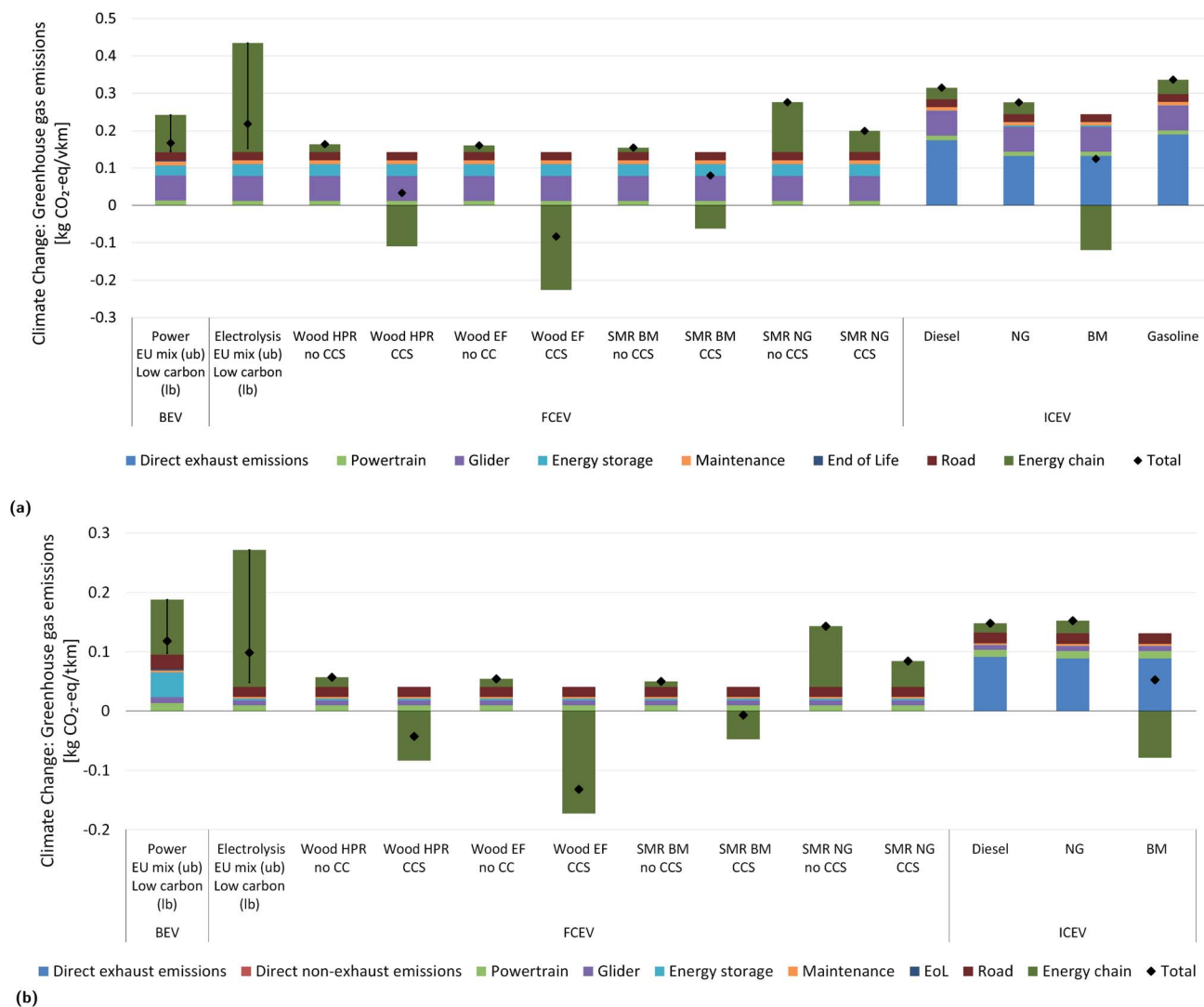
Fig. 11 Climate change impacts including contribution analysis for driving 1 km in a medium size passenger car (a) or transporting 1 ton of goods in a 26 ton truck (b) with varying fuel chains and drivetrains. The portfolio includes FCEV (Fuel Cell Electric Vehicles) driven with H_2 from various sources as presented above; BEV (Battery Electric Vehicles) supplied by an average European electricity mix (corresponding to the upper bound (ub) of the error bar), hydropower (corresponding to the lower bound (lb) of the error bar), and solar PV (corresponding to the "total"); and ICEV (Internal Combustion Engine Vehicles) fuelled by conventional petrol, natural gas (NG) or biomethane (BM), or diesel.

wood-based hydrogen. Paradoxically, lower efficiency of the process compared to reforming pays off in terms of carbon removal from the atmosphere. However, the limited availability of wood chips from sustainable forestry needs to be kept in mind. Fig. 15 also reveals that while the electrolysis process shows high sensitivity to the GHG intensity of the electricity used, climate change impacts of both the reforming as well as the gasification are not driven by the GHG intensity of electricity. Therefore, modelling the electricity input with low-carbon electricity as opposed to our default assumption using the European (ENTSO-E) mix would not change findings on climate change impacts of H_2 from reforming or gasification. However, many other environmental impact categories are influenced by the use of the ENTSO-E mix (see complete set of LCIA results in the ESI†) for all technologies with an

increased electricity use (e.g. HPR, reforming combined with CCS).

Fig. 10 provides LCA results for H_2 production with all woody biomass gasification configurations for a number of selected, representative impact categories (the complete set of results is part of the LCA section in the ESI†). We compare the dry biomass gasification process chains to steam methane reforming and electrolysis with hydro or wind power in each impact category. Each impact category is normalized for the absolute maximum value. This representation allows showing the performance of technologies for a set of chosen environmental impacts in comparison. Hence, it is possible to identify technologies which might potentially perform well in most impact categories, or recognise trade-offs when a technology comes with large improvements in one impact

category compared to less effective technologies, but might trigger high environmental impacts in another category. For instance, an important question in the context of CCS is, if the reduction of climate change impacts comes at substantial increases regarding impacts in other areas of environmental concern.

Neither the use of wood nor addition of CCS result in large additional burdens regarding non-renewable cumulative energy demand, ecosystem quality and human health impacts compared to hydrogen from natural gas and biomethane. The only exception is land use: forestry for wood chips production is associated with forest land use and this dominates the results in the land use category, even if this is simply land used for sustainable forestry. The land use of extensive forestry does not imply any important change in how land is used, as it would be the case if an extensive forest were turned e.g. into an industrial area. The high land occupation value does therefore not indicate a situation, which is environmentally problematic, but simply shows in this case that the use of wood chips as feedstock occupies more square meters of land than other feedstock options for hydrogen production. In comparison, all other hydrogen production technologies do apparently cause substantially less land use. The non-renewable cumulative energy demand is highest for the use of natural gas. In freshwater ecotoxicity, the comparatively high impact of H_2 from wind-based electrolysis is driven by the use of stainless steel for the wind turbines. Sources for emissions to air responsible for photochemical ozone formation are diverse and therefore the burdens in this impact category are driven by the use of natural gas, the wood chips supply chain, use of electricity, or material use (wind electrolysis). In general, results for hydrogen from electrolysis in non-climate change impact categories depend mostly on the source of electricity, even within the portfolio of renewables with e.g. considerable differences between hydropower and photovoltaic power. Therefore, general conclusions for these impact categories comparing hydrogen from electrolysis with biomass-based hydrogen (with and w/o CCS) cannot be drawn.

In order to evaluate the environmental performance of hydrogen from different production pathways from an overall life-cycle perspective, we include the end use. We select the mobility sector and quantify environmental life-cycle burdens of passenger cars and freight transport vehicles in the next section.

5.6 Hydrogen and its role in decarbonization of the transport sector – use of hydrogen in passenger cars and freight trucks

Fig. 11 illustrates the climate change impacts and the contributions of various life cycle phases from driving 1 vehicle-kilometer (vkm) in a medium size passenger car of various drivetrain technologies and fuel supply chains (Fig. 11a), and results for 1 ton-kilometer (tkm) with a 26 ton truck in a regional driving cycle and average load factor, as specified in (Fig. 11b).[19,20] Note that due to the different

functional units the results for passenger vehicles and trucks are not directly comparable. We select conventional Internal Combustion vehicles (ICEV) with diesel, natural gas/biomethane, and petrol, Fuel Cell Electric Vehicles (FCEV) with several hydrogen supply pathways, and battery electric vehicles (BEV) with different electricity supply options. To reduce the set of alternatives for hydrogen production, we only consider steam reforming (SMR) of natural gas (NG) or biomethane (BM)[1] and the HPR and EF configurations from this work. oxySER is the least mature technology represented in this work and is therefore excluded here from application for vehicles. The BM chain selected here corresponds to the pessimistic range assuming low carbon uptake and release of carbon in the digestate of anaerobic biowaste digestion to the atmosphere (i.e. no long-term storage of that carbon in soil).[1]

For passenger vehicles, only using H_2 from wood EF with CCS results in negative life-cycle GHG emissions, while in case of trucks, life-cycle GHG emissions are negative when H_2 from wood HPR and EF with CCS is used. This difference between passenger vehicles and trucks is due to the fact that fuel supply related contributions to life-cycle impacts on climate change of trucks are larger, since the "vehicle utilization" is higher for trucks than for passenger cars. This means that trucks exhibit a larger number of lifetime-kilometers, which leads to lower contributions from vehicle manufacturing and maintenance (corresponding to glider, powertrain, maintenance, energy storage, end-of-life), since the associated emissions are "amortized" over a larger number of kilometers. In general, the use of biomass as feedstock for fuel supply seems to yield substantially reduced climate change impacts compared to fossil fuel ICEV. Using woody biomass results in the highest carbon removal per km driven due to the different H/C ratios of wood and biomethane and to the corresponding process efficiencies. FCEV fuelled with almost all of the analyzed hydrogen production pathways as well as BEV using low-carbon electricity perform (much) better in terms of climate change than current conventional vehicles (ICEV diesel, natural gas or gasoline). An analysis of all other environmental impact categories (see ESI† for the complete set of results) shows that this often does not result in significant negative environmental effects in other impact categories. Wood-based hydrogen supply causes high impacts in the land-use category for FCEV operated with such hydrogen. In addition, battery production for BEV can cause substantial burdens in some impact categories. The use of a carbon intensive electricity mix for charging a BEV or producing H_2 via electrolysis should be avoided due to even higher environmental impacts compared to conventional fuels. Such electricity supply results in high impacts on climate change and in other environmental impact categories, while the use of hydropower is most beneficial in all impact categories. This latter seems to be a sustainable choice when aiming at decarbonization, together with FCEVs driven by H_2 from biomass, be it with or even without CCS. In contrast, the use of conventional fossil-based H_2 from reforming processes without CCS will be

harmful for the climate. Adding CCS with a high capture rate (*i.e.* specific pre-combustion capture unit CO_2 recovery of 98%) is better suited for decarbonization, and the use of biomethane improves the climate performance even further, thus outperforming the direct use of biomethane in a gas vehicle. The use of wood chips exhibits one strong effect compared to other fuels, which is extensive forest land use. The good environmental performance of using wood or wet waste biomass feedstock for hydrogen supply for FCEV raises questions on the availability of these resources, and trade-offs between the necessity to fulfill a service demand (km driven) and minimising climate change impacts. With a given amount of wood feedstock, a larger distance can be driven in passenger cars than in trucks due to lower fuel demand of passenger cars. This effect increases with increasing size of trucks. However, as seen above, the carbon removal from the atmosphere is higher when using the H_2 in a truck than in a passenger car from a life-cycle perspective. In any case, biomass resource availability is limited, and it needs to be carefully evaluated to which use it should be allocated in terms of social, economic, technological and environmental performance.

Comparability of our LCA results with other studies is limited, since our present analysis together with our previous publication[1] represents the first comprehensive LCA of biomass based hydrogen production with CCS and use of this hydrogen as vehicle fuel in the academic literature. Two recent reports from JRC[47] and the European Commission[48] do include some of the hydrogen production pathways we analyzed. However, the JRC report[47] only includes hydrogen from biomethane reforming and their LCA approach for dealing with potentially avoided burdens differs from ours and therefore, comparing LCA results is not meaningful. The report from the European Commission[48] only includes hydrogen production from natural gas *via* SMR with CCS and their LCA results for impacts on climate change per unit of hydrogen produced as similar to ours. Truck sizes in their analysis differ from ours – thus, we have to refrain from comparing LCA results on the level of vehicles.

6 Conclusions

This analysis represents an extension of our earlier techno-environmental assessment of hydrogen production from natural gas and biomethane with carbon capture and storage.[1] We extended the scope (i) by including hydrogen production from woody biomass and (ii) by evaluating the environmental performance of hydrogen use as vehicle fuel in comparison to alternative options, thereby filling important research gaps identified in our previous work.[1] We have performed an integrated techno-environmental analysis of three gasification technologies for H_2 production from woody biomass: (i) the heat pipe reformer (HPR), (ii) the sorption enhanced reforming gasifier (oxySER), and (iii) the entrained flow gasifier (EF), each of these with and without pre-combustion CO_2 capture followed by permanent geological storage (CCS). For this purpose, we have linked detailed

process models of hydrogen production and Life Cycle Assessment (LCA) taking into account all relevant processes from forestry to end-of-life of vehicles. This procedure allows for a quantification of benefits and potential trade-offs of a range of process configurations from both technical and environmental perspectives in a consistent way. Nevertheless, a few simplifications made in this work should be considered more closely in the future:

● Wood gasification is a complex process and the process efficiency strongly depends on the type of feedstock used and on the operating conditions (*e.g.*, residence time, temperature, wood water and impurities content). In this analysis we consider a standard wood composition which is in agreement with the ecoinvent report on wood energy.[35] However, a different feedstock composition might lead to different results (both in terms of process efficiency and type of pre-treatment required), and the wood quality is region specific. Concerning the operating conditions, it is hard to define standard operating conditions because those technologies are at an early stage of development and employment; nevertheless, in a real application the operating conditions of the gasification technologies should be optimized for the specific feedstock composition.

● Product gas cleaning is a key aspect while dealing with biomass gasification, and in a real application it might represent a substantial challenge; the cleaning strategy suggested in the framework of this contribution might not be enough to completely eliminate contaminants as tars. Therefore, additional cleaning step might be required, leading to an increase is pressure drop, process complexity and indirectly also to an increase in costs.

● EF gasifier: given the absence of the steam reformer, instead of removing H_2S from the product gas before the WGS section, the high temperature shift could be replaced by a sour WGS reactor.[49] However, unlike coal gasification (where the sulphur content in the product gas is in the order of thousands ppm), the sulphur content here is from one to two orders of magnitude lower.[21,23,50] Thus, because of the low H_2S content, a sour WGS might not work (*i.e.* to active the catalyst, an H_2S content in the order of thousands ppm is needed[51]). An other consideration we would like to make concerns the type of CO_2 capture considered for the EF CCS chain; other separation technologies than amine-based absorption could be used instead, as for example physical scrubbing. However, the comparison of different types of CO_2 capture technologies goes beyond the scope of this work, thus we decided to use the same capture technology for all production pathways, in order to be able to perform a fair comparison.

● Cooling and heating large amounts of product gas might be challenging in a real application; therefore, the suggested cooling/heating strategy presented in this contribution might have to be changed, affecting not only the heat integration efficiency but also the overall electricity balance of the production chain.

● The sorption enhanced reforming gasifier is the least mature technology among the three. Ideally, to avoid the need

of cooling under water condensation temperature before gas cleaning, the gasification should occur at higher pressure (*e.g.* 5 bar). Since steam is needed in both SMR and WGS reactors, the intermediate condensation of water would cause an efficiency drop, thus it is not convenient to follow a downstream design as the one of the GoBiGas plant.[52] Nevertheless, the goal of this contribution is to verify the potential of different pathways and the characteristics of the product gas generated by this type of gasifier are promising, despite the low stage of technical development.

• Other gasification technologies exist and may be used (in combination with a proper downstream train) to produce hydrogen (*e.g.* oxygen blown fluidized bed and dual fluidized bed gasifier). However, we have decided to select the three above because they allow to compare different features and specifications, crucial to understand which combination could be the most suitable for hydrogen production.

• The LCA proposed here considers woody biomass feedstock for H_2 production from forestry in Germany and Sweden, as considered to be representative for the European wood chips market in the ecoinvent database.[45] However, forestry-related environmental burdens depend on regional boundary conditions and wood markets may differ from region to region. Such differences should be addressed.

• The wood supply chain considered in this analysis represents "sustainable forestry", *i.e.* the use of trees extracted from existing forests in a quantity at or below the natural growth rate. Since the potential of such resources is limited, using wood from dedicated plantations should be analyzed, appropriately reflecting site-specific boundary conditions.

• The quantification of selected environmental burdens in addition to impacts on climate change accounts for the amounts of emitted pollutants, but not for actual damages to human health and ecosystems. Quantifying these impacts would require regionalized or even location-specific impact assessment based upon specific dose-response functions – an issue which would be especially important in the context of mobility, but the LCA community is struggling with.

While acknowledging the limitations above, we are still confident that our analysis provides reliable and useful outcomes, which can be summarized as follows. Regarding hydrogen production, considering both process efficiency and overall environmental performance, the oxySER configurations with CCS exhibits better technical and environmental performances than the other configurations. However, the oxySER process represents the most immature technology among the three configurations analyzed. All three wood-based hydrogen production configurations with CCS result in negative life-cycle GHG emissions, *i.e.* a "net-removal" of CO_2 from the atmosphere due to the permanent storage of CO_2 absorbed by trees; these results are similar to those of biowaste-based biomethane reforming with CCS. The negative GHG emissions of wood-based hydrogen production with CCS do not come with substantial burden-shifting, *i.e.* the production processes are not associated

with high environmental burdens in other impact categories. Land use from forestry is substantial, but this is land occupied by forests used for wood supply chains from sustainable forestry where wood consumption does not exceed natural growth rates. In general, hydrogen from biogenic feedstock used in fuel cell vehicles represents an environmentally sound fuel–powertrain combination, not only in comparison with conventional diesel, petrol and natural gas vehicles, but also in comparison with battery electric vehicles (BEV). Regarding impacts on climate change, FCEV with hydrogen from biomass without CCS exhibit similar or slightly better (depending on the vehicle type) performance as BEV charged with low-carbon electricity. Adding CCS to biomass-based hydrogen production results in substantially lower impacts on climate change of FCEV compared to BEV, and in certain cases even to negative life-cycle GHG emissions per kilometer driven. However, these results require a careful interpretation. First, biomass resources to be used for hydrogen production are limited and can only provide fuel for a minor fraction of current vehicle fleets. And second, negative life-cycle GHG emissions for vehicles on a "per km" basis partially result from inefficient fuel use: if the fuel supply chain exhibits negative GHG emissions, the more fuel a vehicle consumes, the more CO_2 it removes from the atmosphere. More efficient fuel use would increase life-cycle GHG emissions per kilometer, but from a vehicle fleet perspective it would allow for travelling more km with the same amount of fuel and CO_2 removal from the atmosphere. Therefore, increasing the "negativity" of life-cycle GHG emissions of vehicles per km driven by increasing consumption of fuel associated with negative GHG emissions must not be the goal. The results of our analysis clearly demonstrate that biomass-based hydrogen – with and without CCS – must be considered as an environmentally sound transport fuel and that FCEV fuelled with such hydrogen represent an option to substantially reduce road-transport related impacts on climate change without major adverse environmental side-effects, if biomass is either sourced from waste streams or from sustainable forestry. Resource limitations need to be kept in mind though, and therefore, transition to a low-carbon transport system will require further fuel and vehicle options, *e.g.*, low-carbon electricity used for hydrogen production *via* electrolysis, hydrogen from natural gas reforming with CCS, and direct electrification using BEV.

Appendix

Table 3 summarizes the performance of the six biomass to hydrogen production chains. The detail schemes of the production chains are shown in Fig. 12–14. While Fig. 15 shows the life cycle climate change impacts for H_2 production *via* water electrolysis in comparison with the other production technologies discussed in this contribution.

Table 3 Summary of the performance of the six wood to hydrogen chains

Production chain	Biomass input [MW/H$_2$ produced [MW]	η_{net}	El. balance [kWel MW H$_2^{-1}$]	ψ_{CO2}
HPR	1.62 [1.53–1.72]	0.62 ± 0.04	−93 ± −2.6	0
HPR CCS	1.62 [1.53–1.72]	0.62 ± 0.04	−153 ± −1.5	0.574 ± 0.033
oxySER S	1.43 [1.22–1.66]	0.70 ± 0.11	−139 ± −11.2	0.630 ± 0.02
oxySER CCS	1.43 [1.22–1.66]	0.70 ± 0.11	−167 ± −14.2	0.927 ± 0.006
EF	1.84 [1.79–1.89]	0.54 ± 0.013	−73 ± −8.6	0
EF CCS	1.84 [1.79–1.89]	0.54 ± 0.013	−184 ± −8.6	0.976
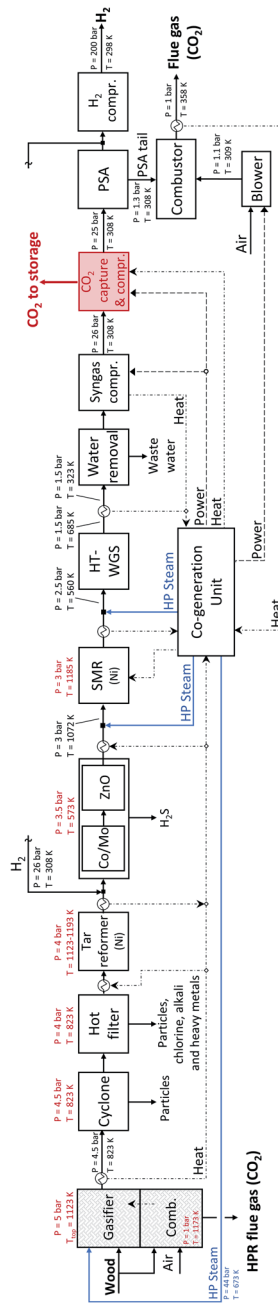
Fig. 12 Detailed scheme of the hydrogen production plant with an HPR gasifier modelled in Aspen Plus.
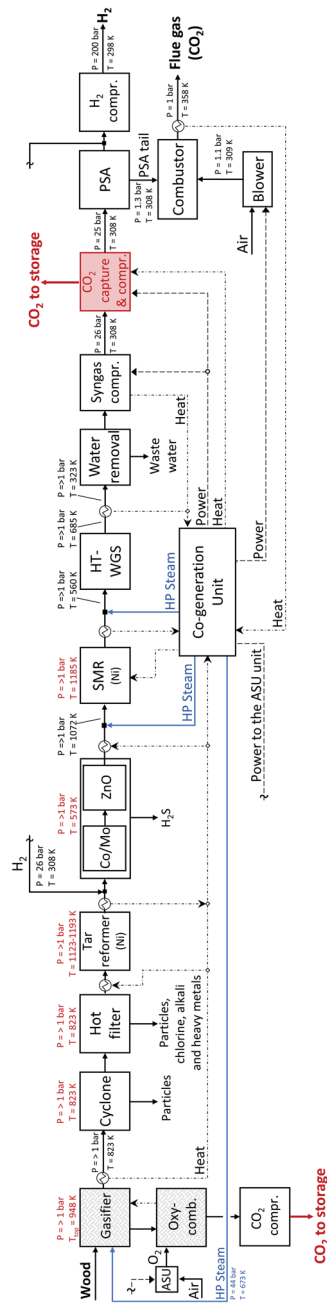
Fig. 13 Detailed scheme of the hydrogen production plant with an oxySER gasifier modelled in Aspen Plus.

Fig. 14 Detailed scheme of the hydrogen production plant with an EF gasifier modelled in Aspen Plus.

Fig. 15 Life cycle climate change impacts for H_2 production *via* water electrolysis, reforming of natural gas (NG) or biomethane (BM), and gasification of wood. A similar figure has already been published in ref. 1 and has now been extended to include the wood gasification configurations. Results are shown in relation to the greenhouse gas intensity of the input electricity to the processes electrolysis, reforming, or gasification, respectively.

Conflicts of interest

There are no conflicts to declare.

Acknowledgements

Notes and references

1 C. Antonini, K. Treyer, A. Streb, M. van der Spek, C. Bauer and M. Mazzotti, *Sustainable Energy Fuels*, 2020, **4**, 2967–2986.

2 M. Allen, M. Babiker, Y. Chen, M. Taylor, P. Tschakert Australia, H. Waisman, R. Warren, P. Zhai, K. Zickfeld, P. Zhai, H. O. Pörtner, D. Roberts, J. Skea, P. Shukla, A. Pirani, W. Moufouma-Okia, C. Péan, R. Pidcock, S. Connors, J. Matthews, Y. Chen, X. Zhou, M. Gomis, E. Lonnoy, T. Maycock, M. Tignor and T. Waterfield, Summary for Policymakers, in *Global Warming of 1.5 °C, an IPCC Special Report on the impacts of global warming of 1.5 °C above pre-industrial levels and related global greenhouse gas emission pathways, in the context of strengthening the global response to, IPCC Technical Report*, 2018.

3 European Commission, *A hydrogen strategy for a climate-neutral Europe. COM(2020) 301 final*, European Commission technical report, 2020.

4 International Energy Agency, *The Future of Hydrogen*, IEA technical report, 2019.

5 A. Sharma and S. K. Arya, *Biotechnol. Rep.*, 2017, **15**, 63–69.

6 H. Tian, J. Li, M. Yan, Y. W. Tong, C. H. Wang and X. Wang, *Appl. Energy*, 2019, **256**, 113961.

7 C. Rodriguez Correa and A. Kruse, *J. Supercrit. Fluids*, 2018, **133**, 573–590.

8 M. Aasadnia and M. Mehrpooya, *Appl. Energy*, 2018, **212**, 57–83.

9 J. Sarkar and S. Bhattacharyya, *Arch. Thermodyn.*, 2012, **33**, 23–40.

10 A. Arregi, M. Amutio, G. Lopez, J. Bilbao and M. Olazar, *Energy Convers. Manage.*, 2018, **165**, 696–719.

11 Y. Gao, J. Jiang, Y. Meng, F. Yan and A. Aihemaiti, *Energy Convers. Manage.*, 2018, **171**, 133–155.

12 K. Sharma, *Renewable Sustainable Energy Rev.*, 2019, **105**, 138–143.

13 M. Luo, Y. Yi, S. Wang, Z. Wang, M. Du, J. Pan and Q. Wang, *Renewable Sustainable Energy Rev.*, 2018, **81**, 3186–3214.

14 W. Khetkorn, R. P. Rastogi, A. Incharoensakdi, P. Lindblad, D. Madamwar, A. Pandey and C. Larroche, *Bioresour. Technol.*, 2017, **243**, 1194–1206.

15 C. Acar and I. Dincer, *J. Cleaner Prod.*, 2019, **218**, 835–849.

16 Y. K. Salkuyeh, B. A. Saville and H. L. MacLean, *Int. J. Hydrogen Energy*, 2018, **43**, 9514–9528.

17 A. Susmozas, D. Iribarren, P. Zapp, J. Linβen and J. Dufour, *Int. J. Hydrogen Energy*, 2016, **41**, 19484–19491.

18 J. B. Guinée, *Life Cycle Assessment: An operational guide to the ISO Standards; LCA in Perspective; Guide; Operational Annex to Guide, Centre for Environmental Science*, Leiden University Technical Report, 2001.

19 R. Sacchi, C. Bauer, B. Cox and C. Mutel, *Renew. Sustain. Energy Rev.*, 2020.

20 R. Sacchi, C. Bauer and B. Cox, *Environ. Sci. Technol.*, 2021, DOI: 10.1021/acs.est.0c07773.

21 G. Gallmetzer, P. Ackermann, A. Schweiger, T. Kienberger, T. Gröbl, H. Walter, M. Zankl and M. Kröner, *Biomass Convers. Biorefin.*, 2012, **2**, 207–215.

22 J. M. Leimert, M. Neubert, P. Treiber, M. Dillig and J. Karl, *Appl. Energy*, 2018, **217**, 37–46.

23 J. Karl, *Biomass Convers. Biorefin.*, 2014, **4**, 1–14.

24 B. Matthias, K. Michael, K. Matthias and L. Markus, *Hydrogen from biomass gasification*, IEA Bioenergy Technical Report, 2018.

25 I. Hannula, *VTT WORKING PAPERS 131 Hydrogen production via thermal gasification of biomass in near-to-medium term Hydrogen production via thermal gasification of biomass in near-to-medium term*, 2009, pp. 1–42.

26 B. Voss, J. Madsen, J. B. Hansen and K. J. Andersson, *The Catalyst Review*, 2016.

27 J. B. Hansen, *presented in part at the IEA Bioenergy Task 33 meeting*, SKIVE, 2017.

28 I. Hannula, Synthetic fuels and light olefins from biomass residues, carbon dioxide and electricity, *Performance and cost analysis*, 2015, p. 118.

29 H. Hermann, R. Reinhard, B. Klaus, K. Reinhard and A. Christian, *Expert Meeting on Pyrolysis and Gasification of Biomass and Waste*, 2002.

30 A. v. Dongen and M. Kanaar, *Co-gasification at the Buggenum IGCC power plant*, Beiträge zur dgmk-fachbereichstagung "energetische nutzung von biomassen" technical report, 2006.

31 O. Font, P. Cordoba, X. Querol, P. Coca and F. Garcia-Peña, *World of Coal Ash Conference*, 2011, pp. 9–12.

32 A. Tremel, D. Becherer, S. Fendt, M. Gaderer and H. Spliethoff, *Energy Convers. Manage.*, 2013, **69**, 95–106.

33 J. C. Meerman, A. Ramírez, W. C. Turkenburg and A. P. Faaij, *Renewable Sustainable Energy Rev.*, 2011, **15**, 2563–2587.

34 C. Wilén and A. Rautalin, *Bioresour. Technol.*, 1993, **46**, 77–85.

35 C. Bauer, *Swiss Centre for Life Cycle*, Inventorie Technical Report, Holzenergie, Paul Scherrer Institute, Villigen, 2007.

36 J. Fuchs, J. Schmid, S. Müller, F. Benedikt, M. Hammerschmid, N. Kieberger, H. Stocker, H. Hofbauer and T. Bürgler, *Optimierung von "Sorption Ehanced Reforming" zur Verbesserung der CO$_2$-Bilanz in der Roheisenerzeugung mittels Biomasse*, Österreichische forschungsförderungsgesellschaft mbh (ffg) Technical Report, 2017.

37 C. Pfeifer, S. Koppatz and H. Hofbauer, *Biomass Convers. Biorefin.*, 2011, **1**, 39–53.

38 Y. Hu, PhD thesis, KTH Royal Institute of Technology, 2011.

39 G. Beysel, *1st International Oxyfuel Combustion Conference*, Cottbus, 2009.

40 M. Manouchehrinejad and S. Mani, *Energy Convers. Manage.: X*, 2019, **1**, 100008.

41 T. Terlouw, C. Bauer, L. Rosa and M. Mazzotti, *Energy Environ. Sci.*, 2021, DOI: 10.1039/d0ee03757e.

42 ISO 14040, *Environmental management - life cycle assessment - principles and framework*, ISO, 2006.

43 ISO 14040, *Environmental management - life cycle assessment - requirements and guidelines*, ISO, 2006.

44 C. Mutel, *J. Open Source Software*, 2017, **2**, 236.

45 G. Wernet, C. Bauer, B. Steubing, J. Reinhard, E. Moreno-Ruiz and B. Weidema, *Int. J. Life Cycle Assess.*, 2016, **21**, 1218–1230.

46 S. Fazio, V. Castellani, S. Sala, E. M. Schau, M. Secchi, L. Zampori and E. Diaconu, *Supporting Information to the Characterisation Factors of Recommended EF Life Cycle Impact Assessment Method: New Models and Differences with ILCD. EUR 28888*, Joint Research Centre (JRC) Technical Report, 2018.

47 M. Prussi, M. Yugo, L. De Prada, M. Padella and M. Edwards, *JEC Well-To-Wheels Report v5*, JRC Science for Policy Report Technical Report, 2020.

48 N. Hill, S. Amaral, S. Morgan-Price, J. Jöhrens, S. Haye, H. Helms, S. Amaral, A. Bauen, N. Abdalla, J. Bates, A. Harris, T. Nokes, E. Cotton, S. Ziem-Milojevic, K. Biemann, H. Fehrenbach, C. Sim, N. Hill and L. German, *Determining the environmental impacts of conventional and alternatively fuelled vehicles through LCA*, European Commission Technical Report 1, 2020.

49 P. Chiesa, S. Consonni, T. Kreutz and R. Williams, *Int. J. Hydrogen Energy*, 2005, **30**, 747–767.

50 B. Rehling, H. Hofbauer, R. Rauch and C. Aichernig, *Biomass Convers. Biorefin.*, 2011, **1**, 111–119.

51 E. P. J. Abbott, F. Martin, A. C. Lara, N. Macleod and E. M. V. Juan Jose Gonzalez Perez, *Water-Gas shift Catalyst*, 2014.

52 H. Thunman, M. Seemann, T. Berdugo Vilches, J. Maric, D. Pallares, H. Ström, G. Berndes, P. Knutsson, A. Larsson, C. Breitholtz and O. Santos, *Energy Sci. Eng.*, 2018, **6**, 6–34.